Research Square

Preprints are preliminary reports that have not undergone peer review.
They should not be considered conclusive, used to inform clinical practice,
or referenced by the media as validated information.

DP71 supports early homeostatic adaptation in DP427-deficient muscle cells

Sylwia Szwec
Adam Mickiewicz University in Poznań
Paulina Kościelniak-Wawro
Adam Mickiewicz University in Poznań
Karolina Dominiak
Adam Mickiewicz University in Poznań
Solmaz Karimi
Adam Mickiewicz University in Poznań
Alicja Durska
Adam Mickiewicz University in Poznań
Ewa Stępniak-Konieczna
University of Life Sciences in Poznań
Patryk Konieczny
patryk.konieczny@amu.edu.pl

Adam Mickiewicz University in Poznań

Research Article

Keywords: Duchenne muscular dystrophy, dystrophin, utrophin, DP71, DP427, UP395, alternative splicing, myogenic differentiation, cytoskeleton

Posted Date: July 24th, 2026

DOI: https://doi.org/10.21203/rs.3.rs-10240031/v1

License: This work is licensed under a Creative Commons Attribution 4.0 International License.
Read Full License

Additional Declarations: No competing interests reported.

Abstract

Background

Duchenne muscular dystrophy (DMD) results from loss of full-length dystrophin (DP427), but many patients retain expression of the short isoform DP71. While DP71 is abundant in proliferating muscle cells and early differentiation stages, its contribution to cellular adaptation in dystrophin-deficient muscle remains poorly understood.

Methods

We analysed *DP71* expression, alternative splicing and promoter activity in human and murine muscle models, and examined the consequences of selective DP427 depletion, complete dystrophin loss, and combined utrophin depletion in differentiating human myotubes. Functional assays were used to assess cell morphology, viability, reactive oxygen species (ROS), intracellular calcium, membrane integrity, and mitochondrial status, while transcriptomic profiling and rescue experiments with individual DP71 splice variants were performed to define isoform-specific mechanisms.

Results

DP71 was enriched in proliferating cells and early myogenic stages and displayed greater splice diversity in human than in murine models. In DP427-deficient myotubes, *DP71* expression increased through enhanced promoter activity rather than increased transcript stability. Retention of DP71 under DP427-deficient conditions was associated with larger myotube areas, improved viability, reduced ROS production, and lower intracellular calcium levels during early differentiation. In contrast, cells lacking all dystrophin isoforms showed more pronounced structural disruption and stress-associated phenotypes. Transcriptomic profiling showed that selective DP427 depletion in cells retaining DP71 produced a state distinct from complete dystrophin deficiency. This state was characterized by weaker induction of structural, extracellular-matrix and stress-responsive genes, together with relative preservation of ribosomal, mitochondrial and proteostasis-related programmes. Functional studies of DP71 splice variants showed differential subcellular localisation and distinct effects on membrane-associated proteins, mitochondrial activity, calcium homeostasis, and cell survival.

Conclusions

DP71 functions as a transcriptionally induced and splice-sensitive modulator of early adaptation in dystrophin-deficient muscle cells. By supporting membrane–cytoskeletal homeostasis and attenuating oxidative and calcium-associated stress, DP71 promotes early cellular resilience but does not restore full

structural maturation. These findings identify retained short dystrophin isoforms as determinants of a distinct early adaptive state and highlight isoform-specific regulation of cellular homeostasis in DMD.

Background

Duchenne muscular dystrophy (DMD) is a severe X-linked disorder caused by mutations in the DMD gene and characterized by progressive skeletal muscle degeneration, cardiomyopathy, and reduced life expectancy [1, 2]. Loss of the full-length dystrophin isoform DP427 disrupts the dystrophin-glycoprotein complex (DGC), compromises sarcolemmal stability, and promotes calcium dysregulation and oxidative stress in muscle, ultimately contributing to myofibre degeneration and impaired regeneration [3, 4]. Although all patients with DMD lack DP427, many retain expression of shorter dystrophin isoforms depending on mutation location [5, 6]. Clinical studies further indicate that patients lacking distal isoforms such as DP71 may display more severe cognitive, growth, and motor phenotypes, suggesting that retained short isoforms could contribute to disease heterogeneity beyond the effects of DP427 loss alone [5, 7–9]. This view is further supported by recent work highlighting the cell-type-specific expression and interaction networks of dystrophin isoforms in the brain, including DP71 and other short isoforms [10].

Among the products of the *DMD* gene, DP71 was originally described as a major short dystrophin product in brain and other non-muscle tissues [11], and is predominantly expressed in proliferating cells and early stages of myogenic differentiation [12–14], whereas DP427 is enriched in mature skeletal muscle, heart, and brain [3, 4]. This developmental switch suggests that DP71 fulfills functions distinct from the structural role of DP427. Previous studies have linked DP71 to cell viability and proliferation [13, 14], cytoskeletal and adhesion-associated organisation [15, 16], mitochondrial and redox-associated functions [13, 17], and membrane-associated complex organisation [18, 19]. In parallel, the dystrophin paralogue utrophin, particularly its full-length isoform UP395, can partially compensate for DP427 deficiency and has therefore been widely explored as a therapeutic substitute in DMD [20–23].

An additional layer of complexity arises from the extensive alternative splicing of DP71 transcripts. Multiple splice variants have been described, particularly involving exons 71–74 and 78, and these variants differ in subcellular localisation and interaction potential [24–26]. Together with previous reports linking DP71 to cytoskeletal and membrane-associated functions [13, 14, 17], these observations raise the possibility that the role of retained DP71 in muscle depends not only on its abundance, but also on the qualitative composition of the expressed splice variants.

Despite these observations, the specific contribution of retained DP71 to the early response of muscle cells to dystrophin deficiency remains poorly defined. In particular, it is unclear whether selective loss of DP427 in the presence of retained DP71 produces merely a weaker form of dystrophin deficiency or instead establishes a distinct adaptive state during early myogenic differentiation. Addressing this question is important for understanding how short dystrophin isoforms influence cellular homeostasis, membrane–cytoskeletal organisation, and transcriptional responses in dystrophin-deficient muscle.

In this study, we tested the hypothesis that DP71 acts as a transcriptionally inducible and splice-sensitive modulator of early adaptation in DP427-deficient muscle cells. We analysed DP71 expression, alternative splicing, and promoter activity in human and murine models, assessed the consequences of selective DP427 loss or complete dystrophin deficiency during myogenic differentiation, and examined the functional properties of individual DP71 splice variants. By integrating molecular, cellular, and transcriptomic approaches, we aimed to determine whether selective loss of DP427 in the presence of retained DP71 is associated with an adaptive state that is molecularly and functionally distinct from complete dystrophin deficiency.

Methods

Animal experiments

Male C57BL/6 mice aged 8–10 weeks were used to analyse *DMD* and *UTRN* expression during muscle regeneration. Muscle injury was induced by intramuscular injection of notexin (NTX) into the extensor digitorum longus (EDL) muscle as described previously [13]. EDLs were collected at defined time points following injury. Noninjected muscles were used as controls. All animal procedures were conducted in accordance with institutional and national regulations governing the use of animals in research, including the Polish Act on the Protection of Animals Used for Scientific or Educational Purposes implementing Directive 2010/63/EU of the European Parliament and of the Council. The study was approved by the Local Ethical Committee for Animal Experimentation in Poznań, Poland (approval no. 56/2020).

Cell culture and myogenic differentiation

Mouse C2C12 myoblasts and human HEK293 and HeLa cells were obtained from ATCC, whereas human primary myoblasts (HSkM) were obtained from Thermo Fisher (A12555), and mouse HL-1 and human AC16 cardiomyocytes were obtained from Sigma-Aldrich (SCC065 and SCC109, respectively). *DMD* knockout HeLa and HEK293 cell lines used in this study were generated and characterized as previously described [13].

Cells were cultured under standard conditions in a humidified incubator at 37°C with 5% CO_2. Myogenic differentiation of HSkM (Fig. S1) and C2C12 cells was induced by serum withdrawal upon reaching high confluence. Differentiation was monitored over several days, and cells were collected at defined time points. Detailed culture conditions and media compositions are provided in Supplementary Methods.

Gene silencing and plasmid transfection

siRNA-mediated knockdown of *DMD* (targeting *DP427, DP71* or total dystrophin transcripts) and *UTRN* was performed using Lipofectamine RNAiMAX according to the manufacturer's protocol. For combined

knockdown experiments, siRNAs were co-transfected at equal concentrations. Overexpression studies were conducted using plasmid vectors encoding FLAG-tagged DP71 splice variants (Fig. S2). Transfections were carried out using appropriate reagents depending on the cell type. Detailed sequences and experimental parameters are provided in Supplementary Table S1 and Supplementary Methods.

DP71 promoter activity and mRNA stability assays

To assess transcriptional regulation of *DP71*, a luciferase reporter construct containing the human *DP71* promoter was used. Cells were co-transfected with firefly and Renilla luciferase constructs, and promoter activity was measured using a dual-luciferase assay system. To evaluate mRNA stability, transcription was inhibited using actinomycin D, and *DP71* mRNA levels were quantified at multiple time points using RT-qPCR. The primer sequences used in this study are listed in Supplementary Table S1.

Molecular analyses

Gene expression was analysed by RT-qPCR via the $2^{-\Delta\Delta Ct}$ method, and alternative splicing patterns were assessed using PCR-based methods. Protein expression and localisation were determined by immunoblotting and immunofluorescence microscopy. Subcellular fractionation was performed using a commercial kit to assess protein distribution across cytoplasmic, membrane, soluble nuclear, chromatin-bound and cytoskeletal compartments. The antibodies used in this study are listed in Supplementary Table S2 and the full membrane immunoblots and gels are shown in Supplementary Original Data.

Functional assays

Cellular phenotypes were assessed using a range of functional assays. Cell viability, apoptosis and proliferation were measured using luminescence-based assays. Plasma-membrane staining, mitochondrial transmembrane potential, mitochondrial level, reactive oxygen species (ROS) production and intracellular calcium levels were quantified using fluorescence-based approaches. All assays were performed in biological replicates using established protocols [13]. Detailed information can be found in Supplementary Methods.

RNA sequencing and bioinformatics analyses

Total RNA from HSkM myotubes was extracted via the Total RNA Zol–OutTM (A&A Biotechnology, 030–100) Kit and RNA Clean & Concentrator–5 with DNase I (Zymo Research, R1014). The quality of the total RNA was evaluated via a TapeStation 2200 with an RNA ScreenTape assay kit (Agilent). Only samples with an RNA integrity number (RIN) ≥ 8 were used for further analyses. HSkM silencing was then confirmed via RT-qPCR analysis. Sample preparation and sequencing data analysis followed the procedures described in [13]. Expression analysis of the *DP71* isoform of the *DMD* gene at the exon level

was performed via the DEXSeq package (version 1.52.0) in the R environment (version 4.4.2). The input data for the analysis were BAM files generated from RNA-seq analysis [27].

Statistical analyses

Statistical significance between groups was assessed using two-tailed unpaired t–tests, with equality of variances evaluated by the F–test. Randomization and blinding were not applied due to the experimental design. The number of analysed EDL muscles and biological replicates (n) is indicated in the figures. For most functional assays, at least five independent biological replicates per condition were used. Immunoblotting experiments were performed using three independent biological replicates for each experiment. Full uncropped blots and corresponding loading controls for all biological replicates are provided in Supplementary Original Data. RT-qPCR data were obtained from biological replicates calculated as the mean of three technical replicates; outliers attributable to technical variability were excluded from analysis.

RNA-seq differential expression analysis was performed using the Wald test with Benjamini–Hochberg correction for multiple testing, and genes with an adjusted p–value (FDR) ≤ 0.05 were considered statistically significant.

All data are presented as mean ± standard deviation (SD). Statistical significance is indicated as *, $p < 0.05$; **, $p < 0.01$; and ***, $p < 0.001$.

Results

DP71 is enriched in foetal tissues and early myogenic stages

We first examined the expression patterns of *DMD* and *UTRN* isoforms across human foetal and adult tissues and cell models (Fig. S3a). *DP71* and *UP395* were the predominant isoforms across most tissues and cell lines, whereas *DP427* expression was enriched in differentiated skeletal muscle, heart, and brain. This distribution is consistent with the established structural role of DP427 in mature tissues [3, 4].

In both human (Figs. 1a, S3b and S4a) and murine (Figs. 1b and S3c, S4b) models, *DP71* levels were highest in undifferentiated tissues and proliferating cells and declined during myogenic differentiation, whereas *DP427* showed the opposite trend. Human-derived cells exhibited higher relative *DP71* levels (Figs. 1a,b, S3c,d and S4a,b) and greater splice variant diversity than murine models (Figs. S4c–f and 1c–e), indicating species-specific regulation. This greater human splice complexity included consistent detection of variants lacking exon 71 and exons 71–74, in addition to the full-length and Δ78-associated forms.

Alternative splicing analysis further revealed that *DP71*Δ78 transcripts predominated in proliferating cells (Figs. S4c–f and 1c–e) and human foetal tissues (Fig. S5), whereas exon 78 inclusion increased during differentiation. Notably, transcripts lacking exon 78 predominated in most proliferating and foetal

contexts, whereas adult skeletal muscle showed preferential representation of exon 78-containing transcripts, further linking exon 78 inclusion to myogenic maturation. In contrast, splicing of exons 71–74 remained relatively stable, indicating that exon 78 exclusion is the primary dynamically regulated splicing event. Together, these findings identify DP71 as a developmentally regulated and splice-diverse dystrophin isoform enriched in early myogenic states, supporting subsequent functional analyses in differentiating human muscle cells.

DP71 is transcriptionally upregulated in response to DP427 and UP395 deficiency

We next examined whether *DP71* expression responds to DP427 loss. Given the species-specific expression patterns, we focused on human cells. Selective depletion of DP427 increased *DP71* expression, and this response was further enhanced by simultaneous utrophin depletion (Figs. S6 and 2a,b). *DP71* upregulation was also observed following *UTRN* silencing alone in both muscle and HeLa cells (Fig. S7), suggesting coordinated regulation of dystrophin and utrophin pathways.

DP71 splicing patterns in differentiated DP427-deficient myotubes resembled those observed in proliferating cells (Figs. 2c and 1c), indicating increased representation of transcripts characteristic of an earlier myogenic stage. However, no increase in transcript stability was observed following actinomycin D treatment (Fig. S8). Instead, elevated *DP71* expression was associated with elevated pre-mRNA levels (Fig. 2d,e) and increased promoter activity (Fig. 2f), supporting transcriptional rather than post-transcriptional regulation. Together, these data show that *DP71* is transcriptionally upregulated in response to DP427 and UP395 deficiency.

DP71 supports early homeostatic adaptation in DP427-deficient myotubes

To assess the functional consequences of *DP71* upregulation, we examined cellular phenotypes in differentiating muscle cells. Myotubes lacking all dystrophin isoforms (si*DMD*) exhibited pronounced cytoskeletal disorganisation and abnormal mitochondrial distribution, whereas myotubes lacking only DP427 (si*DP427*) showed comparatively preserved structural organisation (Fig. 3a). Quantitative analyses further showed that DP427-deficient myotubes displayed larger fibre areas, increased nuclear numbers, and higher viability than si*DMD* myotubes (Fig. 3b–d). These changes were accompanied by reduced ROS production and lower intracellular calcium levels (Fig. 3e,f), indicating a more favourable early homeostatic state under selective DP427 loss.

Importantly, additional depletion of DP71 in DP427-deficient cells abolished these effects and worsened the phenotype (Fig. S9), supporting a contribution of DP71 to early cellular homeostasis. However, increased apoptosis at later stages indicated that DP71 delays rather than prevents cellular deterioration during differentiation. Together, these findings show that retained DP71 supports early adaptation in DP427-deficient myotubes, but does not restore full structural maturation.

DP71 splice variants display distinct localisation and membrane–cytoskeletal properties

We next examined whether DP71 splice variants differ in their subcellular localisation and molecular properties. Immunofluorescence (Fig. 4a) and fractionation (Fig. 4b) analyses indicated that endogenous DP71 proteins localised primarily to the cytoplasm, with variants lacking exon 78 additionally enriched in cytoskeletal and membrane fractions, consistent with splice-dependent compartmentalisation of DP71 proteins. Notably, the localisation of β-dystroglycan and UP395 only partially overlapped with that of DP71, with β-dystroglycan completely absent from the cytoskeletal fraction (Fig. 4b).

To define variant-specific behaviour more directly, we expressed FLAG-tagged DP71 isoforms in dystrophin-deficient human cells. Microscopy analyses confirmed predominant cytoplasmic and membrane localisation of DP71 variants, with constructs lacking exons 71–74 showing a more pronounced membrane-associated distribution (Fig. 4c, arrows). Upon additional *UTRN* silencing, this distribution shifted towards a more cytoplasmic pattern (Fig. 4c). In parallel, immunoblotting analyses showed that variants lacking exons 71–74 were present at lower levels than the corresponding exon-retaining forms (Fig. 5a), indicating reduced protein stability.

We also observed that alternative splicing influenced the relationship of DP71 with membrane-associated proteins. Ectopic expression of *DP71* variants differentially affected UP395 levels (Fig. 5a), whereas all tested variants increased β-dystroglycan abundance to some extent, with the strongest effect observed for DP71Δ71–74Δ78 (Fig. 5b). In contrast, α-syntrophin levels were largely unchanged, with only DP71 and DP71Δ71 partially restoring its abundance (Fig. 5b,c).

Together, these results show that DP71 is a splice-sensitive molecular system rather than a single functional entity. Alternative splicing alters DP71 stability, intracellular distribution, and association with membrane–cytoskeletal components, providing a mechanistic basis for the distinct phenotypic effects of individual variants in dystrophin-deficient cells.

DP71 splice variants differentially regulate membrane integrity, mitochondrial activity, calcium homeostasis, and cell survival

We next examined whether the distinct molecular properties of DP71 splice variants were accompanied by functional differences in dystrophin-deficient cells. All tested variants partially improved plasma membrane integrity and mitochondrial transmembrane potential, although the magnitude of these effects varied between isoforms (Figs. 6a,b). Among the variants examined, DP71Δ71–74Δ78 showed the strongest improvement in membrane-associated readouts and mitochondrial potential, consistent with its pronounced membrane localisation and effect on β-dystroglycan abundance.

In contrast, the variants differed more markedly in their effects on stress-associated phenotypes. Variants lacking exon 78 were associated with increased mitochondrial content, higher ROS production, elevated intracellular calcium levels, and reduced cell numbers relative to exon 78-containing forms (Fig. 7a–e). By comparison, exon 78-containing variants were more effective at limiting calcium accumulation and better preserved cell viability, with the full-length DP71 isoform showing the most favourable effect on cell survival.

These findings indicate that alternative splicing qualitatively shapes DP71 function. While several variants can support selected membrane- or mitochondria-associated properties, their ability to buffer oxidative stress, maintain calcium homeostasis, and sustain cell survival differs substantially. Thus, the biological impact of retained DP71 in dystrophin-deficient cells depends not only on its expression level, but also on the specific splice-variant repertoire present during early differentiation.

Retained DP71 is associated with a distinct transcriptional state in DP427-deficient myotubes

To investigate isoform-specific effects on transcriptional responses in myotubes, we compared conditions with selective DP427 depletion (si*DP427*), characterized by increased DP71 expression, with complete dystrophin deficiency (si*DMD*), as well as their corresponding combinations with utrophin depletion (si*UTRN*) (Figs. S10–S12 and 8; Datasets S1–S6).

Comparison of si*DMD* and si*DP427* myotubes relative to siCtrl indicated that these conditions adopt distinct transcriptional states rather than reflecting different intensities of the same response (Fig. S11a,b; Datasets S1 and S2). Complete dystrophin depletion was associated with strong induction of structural and muscle-related genes, including multiple sarcomeric, contractile, and membrane-linkage components, consistent with a robust compensatory response to structural instability (Fig. S11c; Dataset S1). In contrast, si*DP427* cells showed only partial activation of muscle-specific genes. While selected contractile markers were retained or induced, key maturation- and structure-associated genes were reduced, indicating incomplete functional maturation (Fig. S11c; Dataset S2). Direct comparison of si*DP427* and si*DMD* myotubes further confirmed that the selective DP427-deficient state is transcriptionally separable from complete dystrophin loss (Fig. 8a–d; Dataset S3).

A distinct pattern was observed for genes linked to translation, mitochondrial function, redox balance, and proteostasis. In si*DMD* myotubes, multiple metabolic enzymes, mitochondrial transcripts, and translation-related genes were reduced, consistent with impaired biosynthetic and homeostatic capacity. By contrast, si*DP427* myotubes retained or upregulated a broader set of ribosomal, mitochondrial, redox, and proteostasis-related transcripts, indicating relative preservation of translational and homeostatic functions despite incomplete structural maturation (Figs. S11c and 8b–d; Datasets S1–S3).

In addition to these muscle-intrinsic and homeostatic differences, genes related to ECM organisation and cell adhesion also differed between conditions. Compared with si*DMD* myotubes, si*DP427* cells showed lower expression of multiple ECM- and adhesion-associated genes, consistent with weaker

activation of structural remodelling pathways. Selective DP427 depletion was additionally associated with pronounced suppression of AP-1-like immediate-early response genes *FOS*, *FOSB*, and *EGR1*, indicating attenuation of immediate-early signalling despite retention of selected cytokine- and injury-associated transcripts (Figs. S11c and 8b–d; Datasets S1–S3).

The effects of utrophin silencing were likewise context dependent. The combined si*DMD*/*UTRN* condition retained strong representation of structural and muscle-related genes, but showed marked suppression of interferon- and stress-response genes together with further reduction of selected ECM/adaptation genes. In parallel, the combined si*DP427*/*UTRN* condition showed pronounced repression of structural, differentiation-associated, and ECM-related genes together with continued representation of ribosomal, proteostasis-related, and selected mitochondrial/homeostatic transcripts (Figs. S11c and 8b–d; Datasets S4-S6).

Taken together, these analyses show that complete dystrophin deficiency and selective DP427 depletion are associated with distinct transcriptional states. Compared with complete dystrophin loss, DP427-deficient cells retaining DP71 displayed weaker induction of structural and stress-associated genes, reduced ECM/adhesion-related gene expression, and broader representation of ribosomal, mitochondrial and proteostasis-related transcripts. Additional utrophin depletion did not abolish these differences, but further impaired structural and differentiation-associated gene expression. These findings indicate that retained DP71 is associated with a homeostasis-biased adaptive transcriptional state that remains molecularly distinct from complete dystrophin deficiency.

Discussion

Our findings identify DP71 as a transcriptionally inducible and splice-sensitive contributor to early adaptation in dystrophin-deficient muscle cells. Rather than restoring the full structural role of DP427, retained DP71 was associated with improved early cellular homeostasis, including reduced oxidative stress and calcium dysregulation, preservation of selected biosynthetic and proteostatic programmes, and partial maintenance of cellular organisation during differentiation. At the same time, these effects did not lead to full structural or functional maturation, indicating that early homeostatic resilience and structural differentiation are related but only partially coupled processes under dystrophin deficiency [13–19, 28, 29].

A central feature of the present study is the developmental and isoform-specific context of *DP71* expression. In agreement with previous work, DP71 is most abundant in proliferating cells and early myogenic stages [12, 13], whereas DP427 becomes enriched in mature skeletal muscle, heart, and brain [3, 4]. This stage-dependent shift strongly supports the notion that DP71 fulfils functions distinct from the structural role of DP427 in differentiated fibres. In the current study, selective loss of DP427 increased *DP71* expression, and this response was further enhanced by utrophin depletion. Importantly, the increase in DP71 was associated with enhanced promoter activity and increased pre-mRNA

abundance rather than altered transcript stability, consistent with earlier reports that *DP71* transcription is developmentally regulated and responsive to promoter-level control [12, 30].

Functionally, DP427-deficient myotubes retaining DP71 displayed a more favourable early phenotype than cells lacking all dystrophin isoforms. These myotubes showed preserved cytoskeletal and mitochondrial organisation, increased viability, reduced ROS production, and lower intracellular calcium levels, whereas additional depletion of DP71 worsened the phenotype. These findings support the interpretation that retained DP71 contributes directly to early cellular homeostasis in dystrophin-deficient muscle cells, in line with previous studies linking DP71 to cell viability, mitochondrial function, redox balance, and membrane/cytoskeletal organisation [13–19]. At the same time, the protective effect was not sustained, because apoptosis increased at later stages of differentiation. Thus, DP71 appears to delay rather than prevent cellular deterioration, reinforcing previous evidence that short dystrophin isoforms cannot fully substitute for the architectural role of DP427 in mature muscle [18, 19, 28].

The functional diversity of DP71 splice variants adds an additional layer of regulation. Multiple DP71 splice forms have been described, particularly involving exons 71–74 and 78, and these variants differ in localisation, subcellular distribution, and interaction capacity [24–26, 31–34]. In our analyses, exon composition influenced protein stability, compartmentalisation, and association with membrane–cytoskeletal components. Variants lacking exons 71–74 were less stable and showed reduced relationship with α-syntrophin, whereas exon 78 status strongly influenced localisation and stress-associated phenotypes. These observations are consistent with earlier work indicating that alternative splicing contributes substantially to functional heterogeneity among DP71 proteins and shapes their interaction behaviour with β-dystroglycan- and syntrophin-associated systems [24–26, 31–36].

The splice-variant data further suggest that not all retained DP71 forms are functionally equivalent. Several variants partially improved membrane integrity and mitochondrial transmembrane potential, whereas their effects on ROS, calcium homeostasis, and cell survival differed markedly. In particular, exon 78-containing variants were generally more supportive of calcium control and survival, whereas Δ78-containing variants more often coincided with increased ROS and reduced cell numbers. These findings indicate that DP71 should be viewed not as a single functional entity, but as a splice-sensitive molecular system whose variant composition can shift the balance between membrane support, stress buffering, and cellular fitness [24–26, 31]. The possibility that excessive or dysregulated DP71 activity may become detrimental under some conditions is also consistent with prior observations of dominant-negative or maladaptive effects of short dystrophin isoforms [29].

The transcriptomic analyses reinforce this interpretation at the systems level. Compared with cells lacking all dystrophin isoforms, DP427-deficient cells retaining DP71 showed weaker induction of structural and stress-associated genes, reduced ECM/adhesion-related responses, and broader representation of transcripts linked to ribosomal function, mitochondrial activity, redox balance, and proteostasis. These features are consistent with a homeostasis-biased adaptive state, rather than with full restoration of myogenic maturation. More broadly, this interpretation agrees with previous

transcriptomic work in dystrophic muscle, which has highlighted dysregulation of structural, metabolic, and stress-associated pathways in DMD models and patient material [37–40]. In our dataset, pathway-level analyses further connected the DP71-associated state to processes involving cytoskeleton in muscle cells, ECM–receptor interaction, motor proteins, and focal adhesion, providing a molecular framework for the observed differences in morphology and stress tolerance [41].

The role of utrophin further refines this model. Utrophin, particularly the full-length UP395 isoform, is widely recognised as a functional paralogue of dystrophin that can partially restore DGC organisation and muscle function, which is why it has been extensively explored as a therapeutic substitute in DMD [20–23]. In the present study, additional utrophin depletion did not abolish the distinction between selective DP427 loss and complete dystrophin deficiency, but it did further impair structural and differentiation-associated gene expression. These findings indicate that DP71-dependent adaptation and utrophin-supported structural programmes are mechanistically related but not equivalent. In this framework, utrophin appears to contribute more strongly to structural differentiation-associated transcription, whereas DP71 is linked more closely to preservation of early homeostatic functions. Utrophin-containing membrane complexes in adherent cultured cells further support the idea that dystrophin-related proteins can participate in partially overlapping membrane-associated systems outside mature muscle fibres [42].

From a broader biological perspective, the current results provide a plausible explanation for why retention of short dystrophin isoforms may contribute to disease heterogeneity in DMD. Genotype-dependent preservation of DP71 and other distal isoforms has previously been linked to variation in cognitive, growth, and motor phenotypes [5–9], while splice-variant diversity further suggests that the consequences of retaining DP71 depend not only on its presence, but also on the specific variant repertoire expressed [24–26]. Our data support a model in which complete dystrophin loss triggers a stronger structural and stress-associated response, whereas selective loss of DP427 in the presence of DP71 is associated with a distinct adaptive state characterised by partial preservation of homeostatic capacity and incomplete structural maturation. Such a framework helps reconcile how retained short isoforms may improve early cellular resilience without being sufficient to maintain long-term muscle integrity [5–9, 24–26].

This study has several limitations. Most importantly, the conclusions are based primarily on in vitro cell models, and although the expression analyses were supported by human and murine developmental contexts, further in vivo validation will be required to define the temporal dynamics of DP71 induction, its interaction with utrophin-dependent compensation, and its impact on regeneration and disease progression in intact muscle. In addition, variant-specific effects were examined largely by ectopic expression in cultured cells, which may not fully reproduce endogenous stoichiometry or tissue context. The data also suggest that some variants may become detrimental when expressed at inappropriate levels, a possibility that is consistent with previous reports indicating potentially adverse effects of excessive DP71 activity [29].

Despite these limitations, the study has clear conceptual implications. Current DMD strategies have focused largely on DP427 restoration, utrophin upregulation, and systemic approaches aimed at modifying body-wide disease manifestations, whereas the present data indicate that DP71-mediated adaptation may represent an additional layer of isoform-specific regulation that shapes the early cellular response to dystrophin deficiency [21, 43–47]. In this context, modulation of *DP71* expression or splicing may be relevant not as a substitute for full structural restoration, but as a means of influencing early cellular resilience and homeostatic capacity. This possibility should, however, be approached cautiously, given the pronounced splice-dependent functional heterogeneity observed here and the likelihood that some variants may be less beneficial than others. Combination dystrophin/utrophin approaches may also prove informative in this setting, as coordinated expression of related isoforms can provide additive functional benefit in dystrophic muscle [46, 48].

In summary, our results identify DP71 as a stage-specific, transcriptionally inducible, and splice-sensitive regulator of early adaptation in dystrophin-deficient muscle cells. By supporting membrane–cytoskeletal homeostasis, limiting oxidative and calcium-associated stress, and preserving selected biosynthetic and proteostatic programmes, DP71 promotes an early adaptive state that is molecularly distinct from complete dystrophin deficiency. However, these effects do not restore full structural maturation, indicating that homeostatic adaptation and structural differentiation are separable outcomes of dystrophin isoform loss. Together, these findings provide a cellular framework that may help explain how retention of short dystrophin isoforms contributes to disease heterogeneity in DMD.

Conclusions

DP71 functions as a transcriptionally induced and splice-sensitive contributor to early adaptation in DP427-deficient muscle cells. Retained DP71 attenuates oxidative and calcium-associated stress, supports selected membrane-associated and homeostatic features, and preserves aspects of mitochondrial, translational and proteostatic activity during early differentiation. However, DP71 does not restore DP427-dependent structural maturation, indicating that homeostatic resilience and full myogenic structural differentiation are separable outcomes of dystrophin isoform loss. These findings identify retained short dystrophin DP71 as a determinant of an early adaptive state in dystrophin-deficient muscle cells and provide a framework for understanding isoform-dependent variability in DMD pathology.

Abbreviations

AC16
human cardiomyocyte cell line AC16
C2C12
murine myoblast cell line C2C12
DGC
dystrophin-glycoprotein complex

DMD
Duchenne muscular dystrophy
DMD gene
dystrophin gene
DP71
short (71 kDa) dystrophin isoform
DP427
full-length (427 kDa) dystrophin isoform
ECM
extracellular matrix
EDL
extensor digitorum longus
FDR
false discovery rate
FLAG
FLAG epitope tag
GEO
Gene Expression Omnibus
GO
Gene Ontology
HEK293
human embryonic kidney 293 cells
HeLa
human cervical carcinoma cell line HeLa
HSkM
human skeletal muscle cells
KEGG
Kyoto Encyclopedia of Genes and Genomes
ko
knockout
NTX
notexin
RF
relative fluorescence
RL
relative luminescence
RIN
RNA integrity number
RNA-seq
RNA sequencing

ROS
reactive oxygen species
RT-qPCR
reverse transcription quantitative PCR
SD
standard deviation
siCtrl
control small interfering RNA
si*DMD*
small interfering RNA targeting total dystrophin transcripts
si*DP427*
small interfering RNA targeting DP427 transcripts
siRNA
small interfering RNA
si*UTRN*
small interfering RNA targeting *UTRN* transcripts
UP395
full-length (395 kDa) utrophin isoform
UTRN
utrophin gene
wt
wild-type

Declarations

Ethics approval and consent to participate

All animal procedures were conducted in accordance with institutional and national regulations governing the use of animals in research, including the Polish Act on the Protection of Animals Used for Scientific or Educational Purposes implementing Directive 2010/63/EU of the European Parliament and of the Council. The study was approved by the Local Ethical Committee for Animal Experimentation in Poznań, Poland (approval no. 56/2020). All efforts were made to minimize animal suffering and to reduce the number of animals used.

Human primary skeletal muscle cells and human tissue-derived cDNA samples were obtained from commercial sources and used in accordance with the suppliers' ethical and consent documentation. No identifiable human data were used in this study.

Consent for publication

Not applicable.

Availability of data and materials

The RNA-seq datasets generated during the current study are available in the Gene Expression Omnibus (GEO) repository under accession number GSE303672: https://www.ncbi.nlm.nih.gov/geo/query/acc.cgi?acc=GSE303672.

Competing interests

The authors declare no competing interests.

Funding

This study was supported by the Polish National Science Centre (NCN) grant Nos. 2018/30/E/NZ5/00065 (to PK), 2021/43/B/NZ5/00723 (to PK), 2020/37/B/NZ5/01263 (to ESK), and 2022/46/E/NZ5/00088 (to ESK).

Authors' contributions

Conceptualization: PK, SS; Methodology: PK, SS, PKW; Investigation, Data curation, Formal analysis and Visualization: SS, PKW, KD, SK, AD, PK, ESK; Funding acquisition: PK, ESK; Project administration: PK; Supervision: PK; Writing – original draft: SS, PK, PKW; Writing – review & editing: PK, with contributions from PKW, SK, ESK. All authors read and approved the final manuscript.

Acknowledgments

Not applicable.

References

1. Bushby K, Finkel R, Birnkrant DJ, Case LE, Clemens PR, Cripe L, Kaul A, Kinnett K, McDonald C, Pandya S, Poysky J, Shapiro F, Tomezsko J, Constantin C. and D. M. D. C. C. W. Group Diagnosis and management of Duchenne muscular dystrophy, part 2: implementation of multidisciplinary care Lancet Neurol *9* (2010) 177–89. 10.1016/S1474-4422(09)70272-8
2. Zhang Y, Mann JR, James KA, McDermott S, Conway KM, Paramsothy P, Smith T, Cai B. and M. D. STARnet Duchenne and Becker Muscular Dystrophies' Prevalence in MD STARnet Surveillance Sites: An Examination of Racial and Ethnic Differences Neuroepidemiology *55* (2021) 47–55. 10.1159/000512647
3. Starosta A. Konieczny Therapeutic aspects of cell signaling and communication in Duchenne muscular dystrophy Cell. Mol Life Sci. 2021;78:4867–91. 10.1007/s00018-021-03821-x.
4. Belhasan DC. and M. Akaaboune The role of the dystrophin glycoprotein complex on the neuromuscular system Neurosci Lett *722* (2020) 134833. 10.1016/j.neulet.2020.134833
5. Matsumoto M, Awano H, Lee T, Takeshima Y, Matsuo M. and K. Iijima Patients with Duchenne muscular dystrophy are significantly shorter than those with Becker muscular dystrophy, with the

higher incidence of short stature in Dp71 mutated subgroup Neuromuscul Disord *27* (2017) 1023–8. 10.1016/j.nmd.2017.06.007

6. Tuffery-Giraud S, Beroud C, Leturcq F, Yaou RB, Hamroun D, Michel-Calemard L, Moizard MP, Bernard R, Cossee M, Boisseau P, Blayau M, Creveaux I, Guiochon-Mantel A, de Martinville B, Philippe C, Monnier N, Bieth E, Khau P, Van Kien FO, Desmet V, Humbertclaude JC, Kaplan J, Chelly. and M. Claustres Genotype-phenotype analysis in 2,405 patients with a dystrophinopathy using the UMD-DMD database: a model of nationwide knowledgebase Hum Mutat *30* (2009) 934–45. 10.1002/humu.20976
7. Doorenweerd N, Mahfouz A, van Putten M, Kaliyaperumal R, PAC TH, Hendriksen JGM, Aartsma-Rus AM, Verschuuren J, Niks EH, Reinders MJT. Kan and B. P. F. Lelieveldt Timing and localization of human dystrophin isoform expression provide insights into the cognitive phenotype of Duchenne. muscular dystrophy Sci Rep. 2017;7:12575. 10.1038/s41598-017-12981-5.
8. Ricotti V, Mandy WP, Scoto M, Pane M, Deconinck N, Messina S, Mercuri E, Skuse DH. Muntoni Neurodevelopmental, emotional, and behavioural problems in Duchenne muscular dystrophy in relation to underlying dystrophin gene mutations. Dev Med Child Neurol. 2016;58:77–84. 10.1111/dmcn.12922.
9. Chesshyre M, Ridout D, Hashimoto Y, Ookubo Y, Torelli S, Maresh K, Ricotti V, Abbott L, Gupta VA, Main M, Ferrari G, Kowala A, Lin YY, Tedesco FS, Scoto M, Baranello G, Manzur A. Aoki and F. Muntoni Investigating the role of dystrophin isoform deficiency in motor function in Duchenne muscular dystrophy. J Cachexia Sarcopenia Muscle. 2022;13:1360–72. 10.1002/jcsm.12914.
10. Tetorou K, Aghaeipour A, Singh S, Morgan JE. and F. Muntoni The role of dystrophin isoforms and interactors in the brain Brain *148* (2025) 1081–98. 10.1093/brain/awae384
11. Lederfein D, Levy Z, Augier N, Mornet D, Morris G, Fuchs O, Yaffe D, Nudel U. A 71-kilodalton protein is a major product of the Duchenne muscular dystrophy gene in brain and other nonmuscle tissues. Proc Natl Acad Sci U S A. 1992;89:5346–50. 10.1073/pnas.89.12.5346.
12. de Leon MB, Montanez C, Gomez P, Morales-Lazaro SL, Tapia-Ramirez V, Valadez-Graham V, Recillas-Targa F, Yaffe D. Nudel and B. Cisneros Dystrophin Dp71 expression is down-regulated during myogenesis: role of Sp1 and Sp3 on the Dp71 promoter activity. J Biol Chem. 2005;280:5290–9. 10.1074/jbc.M411571200.
13. Szwec S, Durska A, Koscielniak-Wawro P, Chamberlain JS, Ostrovskyy O, Dominiak K. Karimi and P. Konieczny Dystrophins DP71 and DP427 determine cell viability during proliferation and myofibre differentiation. Cell Death Dis. 2026;17. 10.1038/s41419-026-08725-x.
14. Farea M, Rani AQM, Maeta K, Nishio H. Matsuo Dystrophin Dp71ab is monoclonally expressed in human satellite cells and enhances proliferation of myoblast cells. Sci Rep. 2020;10:17123. 10.1038/s41598-020-74157-y.
15. Cerna J, Cerecedo D, Ortega A, Garcia-Sierra F, Centeno F, Garrido E, Mornet D. Cisneros Dystrophin Dp71f associates with the beta1-integrin adhesion complex to modulate PC12 cell adhesion. J Mol Biol. 2006;362:954–65. 10.1016/j.jmb.2006.07.075.

16. Howard PL, Klamut HJ. and P. N. Ray Identification of a novel actin binding site within the Dp71 dystrophin isoform FEBS Lett *441* (1998) 337–41. 10.1016/s0014-5793(98)01566-x
17. Lim KRQ, Shah MNA, Woo S, Wilton-Clark H, Zhabyeyev P, Wang F, Maruyama R. Oudit and T. Yokota Natural History of a Mouse Model Overexpressing the Dp71 Dystrophin Isoform. Int J Mol Sci. 2021;22. 10.3390/ijms222312617.
18. Cox GA, Sunada Y, Campbell KP. and J. S. Chamberlain Dp71 can restore the dystrophin-associated glycoprotein complex in muscle but fails to prevent dystrophy Nat Genet *8* (1994) 333–9. 10.1038/ng1294-333
19. Greenberg DS, Sunada Y, Campbell KP, Yaffe D. and U. Nudel Exogenous Dp71 restores the levels of dystrophin associated proteins but does not alleviate muscle damage in mdx mice Nat Genet *8* (1994) 340–4. 10.1038/ng1294-340
20. Li D, Bareja A, Judge L, Yue Y, Lai Y, Fairclough R, Davies KE. Chamberlain and D. Duan Sarcolemmal nNOS anchoring reveals a qualitative difference between dystrophin and utrophin. J Cell Sci. 2010;123:2008–13. 10.1242/jcs.064808.
21. Wu R, Li P, Xiao P, Zhang S, Wang X, Liu J, Sun W, Chang Y, Ai X, Chen L, Zhuo Y, Wang J, Wang Z, Li S, Li Y, Ji W, Guo W, Wu S. Chen Activation of endogenous full-length utrophin by MyoAAV-UA as a therapeutic approach for Duchenne muscular dystrophy. Nat Commun. 2025;16:2398. 10.1038/s41467-025-57831-5.
22. Soblechero-Martin P, Lopez-Martinez A, de la Puente-Ovejero L, Vallejo-Illarramendi A. and V. Arechavala-Gomeza Utrophin modulator drugs as potential therapies for Duchenne and Becker muscular dystrophies Neuropathol Appl Neurobiol *47* (2021) 711–23. 10.1111/nan.12735
23. Loboda A, Chamberlain JS. Dulak Genetic strategies for therapy of Duchenne muscular dystrophy. Mol Ther Nucleic Acids. 2025;36:102759. 10.1016/j.omtn.2025.102759.
24. Naidoo M. and K. Anthony Dystrophin Dp71 and the Neuropathophysiology of Duchenne Muscular Dystrophy Mol Neurobiol *57* (2020) 1748–67. 10.1007/s12035-019-01845-w
25. Alamillo-Iniesta A, Velez-Aguilera G, Monterrubio-Ledezma F, Avila-Aviles RD, Suarez-Sanchez R, Garcia-Aguirre I, Lizcano-Meneses S, Lopez-Orona TI, Guevara-Namorado F, Toribio-Valdez A, Hernandez-Hernandez JM, Arrieta-Cruz I. J. J. Magana and B. Cisneros The molecular mechanism underlying the differential subcellular distribution of dystrophin Dp71 isoforms Cell Biosci *16* (2026). 10.1186/s13578-026-01566-3
26. Gonzalez-Reyes M, Aragon J, Sanchez-Trujillo A, Rodriguez-Martinez G, Duarte K, Eleftheriou E, Barnier JV, Naquin D, Thermes C, Romo-Yanez J, Roger JE, Rendon A, Vaillend C. and C. Montanez Expression of Dystrophin Dp71 Splice Variants Is Temporally Regulated During Rodent Brain Development Mol Neurobiol *61* (2024) 10883–900. 10.1007/s12035-024-04232-2
27. Anders S, Reyes A. and W. Huber Detecting differential usage of exons from RNA-seq data Genome Res *22* (2012) 2008–17. 10.1101/gr.133744.111
28. Harper SQ, Hauser MA, DelloRusso C, Duan D, Crawford RW, Phelps SF, Harper HA, Robinson AS, Engelhardt JF, Brooks SV. Chamberlain Modular flexibility of dystrophin: implications for gene

therapy of Duchenne muscular. dystrophy Nat Med. 2002;8:253–61. 10.1038/nm0302-253.

29. Leibovitz S, Meshorer A, Fridman Y, Wieneke S, Jockusch H. D. Yaffe and U. Nudel Exogenous Dp71 is a dominant negative competitor of dystrophin in skeletal muscle Neuromuscul Disord *12* (2002) 836–44. 10.1016/s0960-8966(02)00141-4
30. Penuelas-Urquides K, Becerril-Esquivel C, Mendoza-de-Leon LC, Silva-Ramirez B, Davila-Velderrain J, Cisneros B. and M. B. de Leon Transcription factors YY1, Sp1 and Sp3 modulate dystrophin Dp71 gene expression in hepatic cells Biochem J *473* (2016) 1967–1976. 10.1042/BCJ20160163
31. Rau F, Laine J, Ramanoudjame L, Ferry A, Arandel L, Delalande O, Jollet A, Dingli F, Lee KY, Peccate C, Lorain S, Kabashi E, Athanasopoulos T, Koo T, Loew D, Swanson MS, Le Rumeur E, Dickson G, Allamand V. J. Marie and D. Furling Abnormal splicing switch of DMD's penultimate exon compromises muscle fibre maintenance in myotonic dystrophy Nat Commun *6* (2015) 7205. 10.1038/ncomms8205
32. Marquez FG, Cisneros B, Garcia F, Ceja V, Velazquez F, Depardon F, Cervantes L, Rendon A, Mornet D, Rosas-vargas H, Mustre M. and C. Montanez Differential expression and subcellular distribution of dystrophin Dp71 isoforms during differentiation process Neuroscience *118* (2003) 957–66. 10.1016/s0306-4522(03)00063-0
33. Austin RC, Howard PL, D'Souza VN. H. J. Klamut and P. N. Ray Cloning and characterization of alternatively spliced isoforms of Dp71 Hum Mol Genet *4* (1995) 1475–83. 10.1093/hmg/4.9.1475
34. Aragon J, Martinez-Herrera A, Romo-Yanez J, Ceja V, Azotla-Vilchis C, Siqueiros-Marquez L, Soid-Raggi G, Herrera-Salazar A. Montanez Identification of Dp71 Isoforms Expressed in PC12 Cells: Subcellular Localization and Colocalization with beta-Dystroglycan and alpha1-Syntrophin. J Mol Neurosci. 2016;58:201–9. 10.1007/s12031-015-0657-8.
35. Jung D, Yang B, Meyer J, Chamberlain JS. Campbell Identification and characterization of the dystrophin anchoring site on beta-dystroglycan. J Biol Chem. 1995;270:27305–10. 10.1074/jbc.270.45.27305.
36. Suzuki A, Yoshida M. Ozawa Mammalian alpha 1- and beta 1-syntrophin bind to the alternative splice-prone region of the dystrophin COOH terminus. J Cell Biol. 1995;128:373–81. 10.1083/jcb.128.3.373.
37. Rizzo B, Dragoni F, Dainesi MI, Di Gerlando R, Minucchi E, Berardinelli AL. Gagliardi Comparative Transcriptomic Profiling in Patients Affected by Duchenne and Becker Muscular Dystrophies: A Focus on ECM Genes Dysregulation. Int J Mol Sci. 2025;26. 10.3390/ijms26146594.
38. Petrany MJ, Swoboda CO, Sun C, Chetal K, Chen X, Weirauch MT. N. Salomonis and D. P. Millay Single-nucleus RNA-seq identifies transcriptional heterogeneity in multinucleated skeletal myofibers Nat Commun *11* (2020) 6374. 10.1038/s41467-020-20063-w
39. Chemello F, Wang Z, Li H, McAnally JR, Liu N, Bassel-Duby R. Olson Degenerative and regenerative pathways underlying Duchenne muscular dystrophy revealed by single-nucleus RNA sequencing. Proc Natl Acad Sci U S A. 2020;117:29691–701. 10.1073/pnas.2018391117.

40. Casati SR, Cervia D, Roux-Biejat P, Moscheni C, Perrotta C. and C. De Palma Mitochondria and Reactive Oxygen Species: The Therapeutic Balance of Powers for Duchenne Muscular Dystrophy Cells *13* (2024). 10.3390/cells13070574
41. Wilson DGS, Tinker A. and T. Iskratsch The role of the dystrophin glycoprotein complex in muscle cell mechanotransduction Commun Biol *5* (2022) 1022. 10.1038/s42003-022-03980-y
42. James M, Nguyen TM, Wise CJ, Jones GE. and G. E. Morris Utrophin-dystroglycan complex in membranes of adherent cultured cells Cell Motil Cytoskeleton *33* (1996) 163–174. DOI: 10.1002/(SICI)1097-0169(1996)33:3<163::AID-CM1>3.0.CO;2-C.
43. Bonnemann CG, Belluscio BA, Braun S, Morris C, Singh T. Muntoni Dystrophin Immunity after Gene Therapy for Duchenne's Muscular Dystrophy. N Engl J Med. 2023;388:2294–6. 10.1056/NEJMc2212912.
44. Tasfaout H, Halbert CL, McMillen TS, Allen JM, Reyes TR, Flint GV, Grimm D, Hauschka SD, Regnier M. and J. S. Chamberlain Split intein-mediated protein trans-splicing to express large dystrophins Nature *632* (2024) 192–200. 10.1038/s41586-024-07710-8
45. Roberts TC, Wood MJA. Davies Therapeutic approaches for Duchenne muscular dystrophy. Nat Rev Drug Discov. 2023;22:917–34. 10.1038/s41573-023-00775-6.
46. Szwec S, Kaplucha Z, Chamberlain JS. and P. Konieczny Dystrophin- and Utrophin-Based Therapeutic Approaches for Treatment of Duchenne Muscular Dystrophy: A Comparative Review BioDrugs *38* (2024) 95–119. 10.1007/s40259-023-00632-3
47. P. Konieczny Systemic Treatment of Body-Wide Duchenne Muscular Dystrophy Symptoms Clin Pharmacol Ther *116* (2024) 1472–84. 10.1002/cpt.3363
48. Guiraud S, Edwards B, Babbs A, Squire SE, Berg A, Moir L, Wood MJ. Davies The potential of utrophin and dystrophin combination therapies for Duchenne muscular dystrophy. Hum Mol Genet. 2019;28:2189–200. 10.1093/hmg/ddz049.

Figures

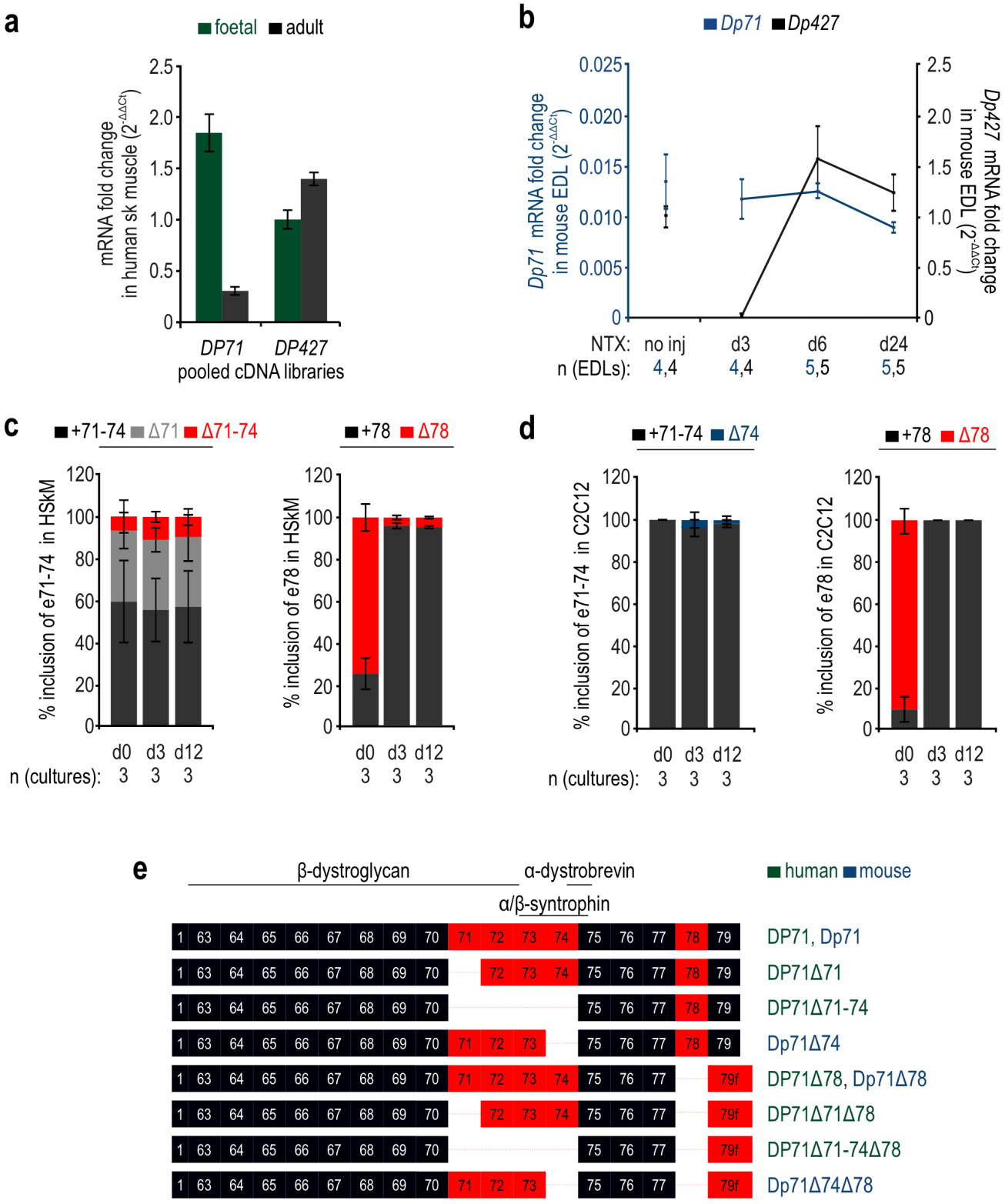


Figure 1

***DP71* shows more complex expression patterns in human than in murine models.**

(a, b) RT-qPCR analyses of *DP71* and *DP427*mRNAs in foetal and adult skeletal muscles (**a**) and EDL muscles at different time points following NTX injection (**b**).

(c, d) Quantification of exon 71–74 and exon 78 inclusion in human HSkM (**c**) and murine C2C12 (**d**) cells at different time points during myotube formation.

(e) Schematic representation of DP71 splice variants identified in human and murine models based on splicing analyses, including binding sites for b-dystroglycan, a/b-syntrophin, and a-dystrobrevin.

The data are presented as mean ± SD. n, number of biological replicates.

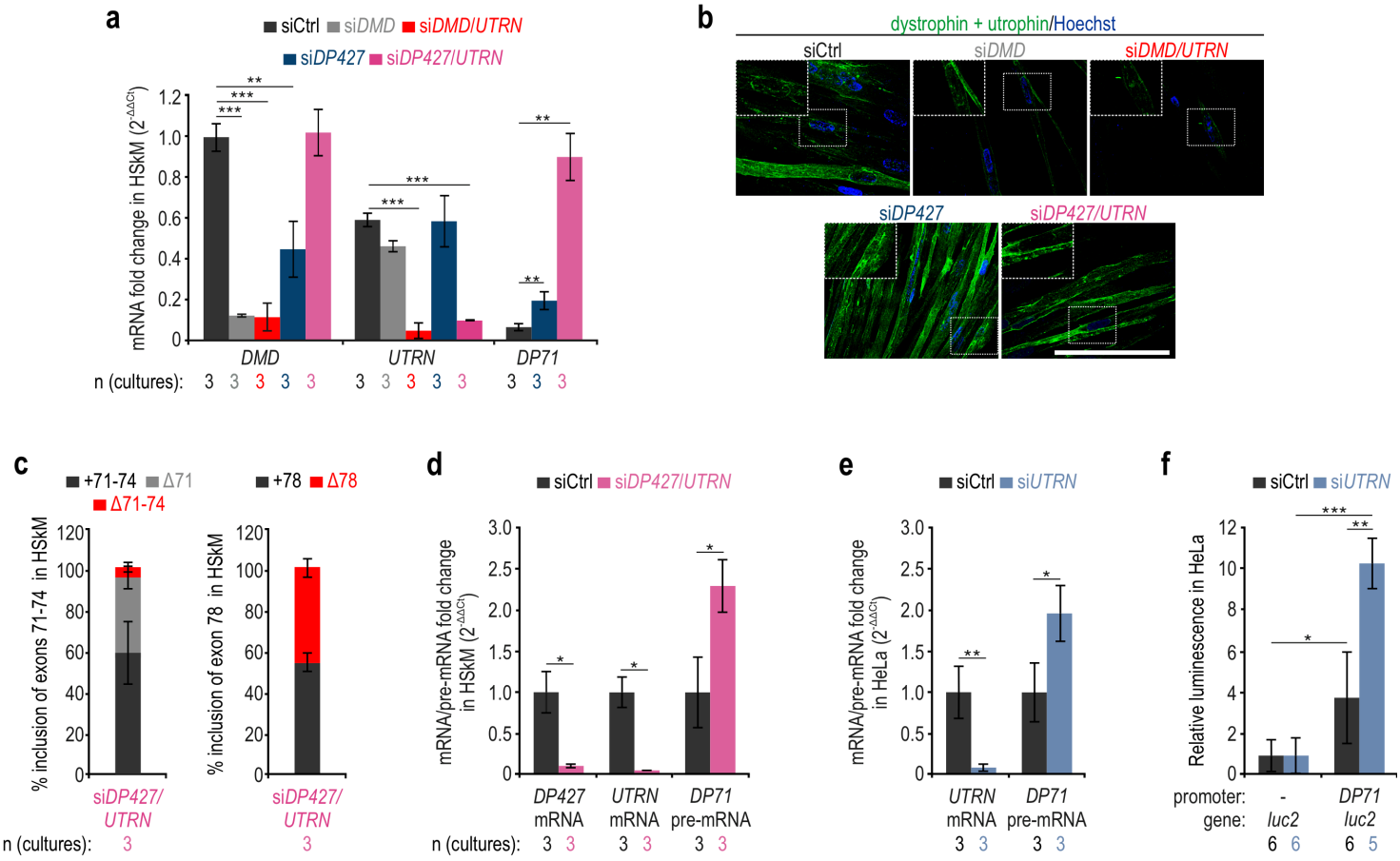


Figure 2

DP71 expression increases in cells deficient in DP427 and/or utrophin (UP395).

(a–b) RT-qPCR (**a**) and immunofluorescence (**b**) analyses of *DMD* and *UTRN* expression in differentiated (d9) HSkM cells following siRNA-mediated knockdown. Microscopy images were generated from six separate pictures taken at various z–positions with the same parameters for each image. Scale bar in **b**: 100 µm.

(c) Quantification of exon 71–74 and 78 inclusions in differentiated HSkM cells under DP427- and utrophin-deficient conditions.

(**d**, **e**) RT-qPCR analyses of mRNA and pre-mRNA levels in siRNA-treated HSkM myotubes (**d**) and HeLa cells (**e**).

(f) *DP71* promoter activity assessed by dual-luciferase assay in HeLa cells following siRNA delivery.

The data are presented as mean ± SD. n, number of biological replicates. *, p < 0.05; **, p < 0.01; ***, p < 0.001 (two-tailed unpaired t–test).

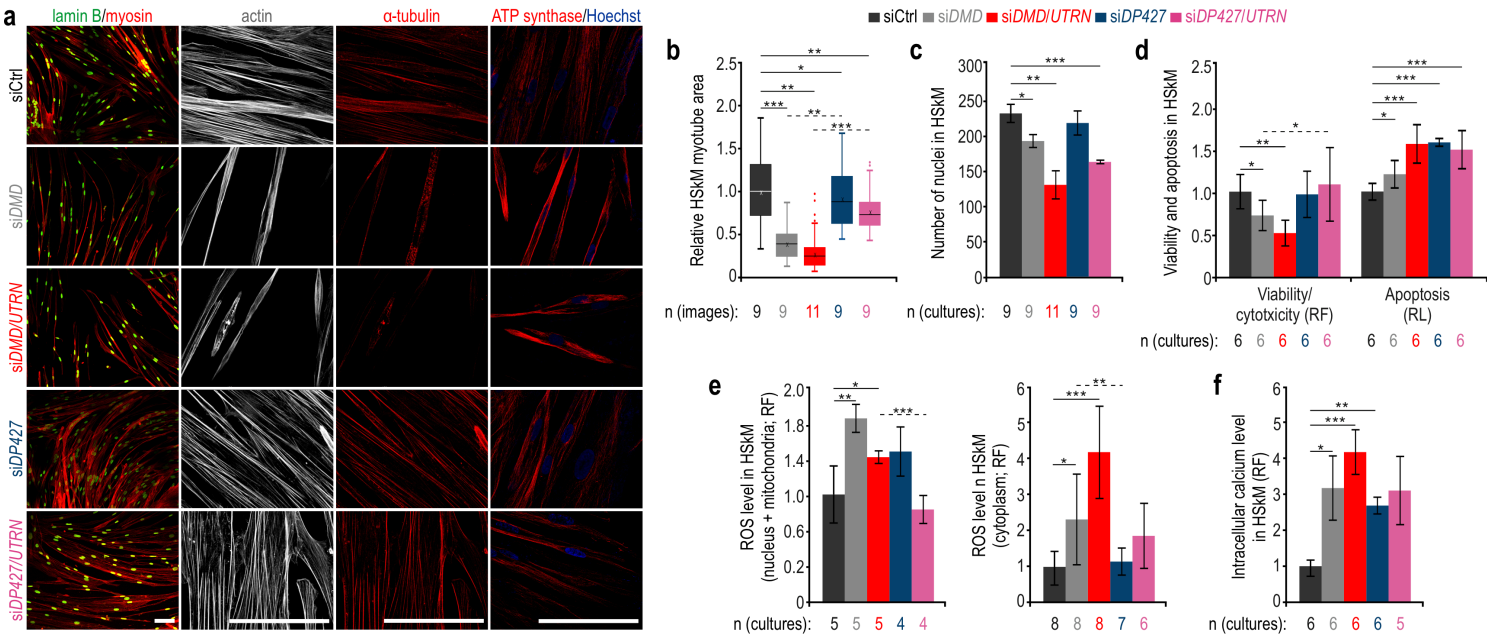


Figure 3

DP71 supports early cellular homeostasis in DP427-deficient myotubes.

(a) Immunofluorescence analysis of differentiated HSkM cells (d9) following depletion of dystrophin isoforms, stained for lamin B, myosin, actin, tubulin, ATP synthase, and nuclei (Hoechst). The images were generated from six separate pictures taken at various z–positions with the same parameters for each image. Scale bars: 100 µm.

(b–d) Quantification of myotube areas (**b**) and nuclear numbers (**c**) at d9 of differentiation, and viability and apoptosis (**d**) at d12 of differentiation in siRNA-treated HSkM myotubes.

(e, f) Quantification of ROS levels (**e**) and intracellular calcium levels (**f**) in differentiated HSkM myotubes (d9) after siRNA treatment.

The data are presented as mean ± SD. RF, relative fluorescence; RL, relative luminescence; n, number of biological replicates. *, p < 0.05; **, p < 0.01; ***, p < 0.001 (two-tailed unpaired t–test).

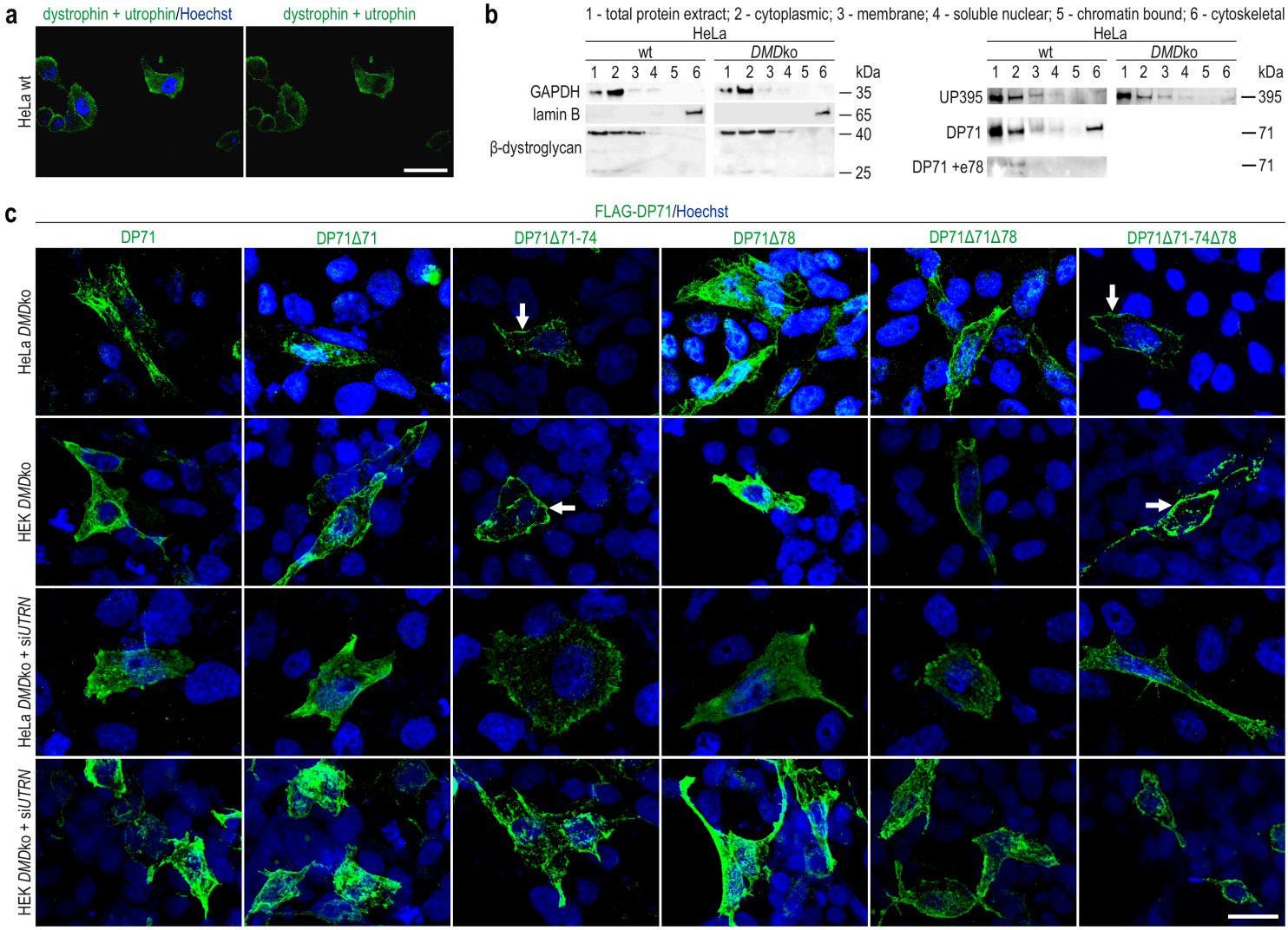


Figure 4

DP71 localisation depends on alternative splicing and *UTRN* status.

(a) Immunofluorescence analysis of wild-type HeLa cells stained for dystrophin (DP71) and utrophin (UP395).

(b) Immunoblot analysis of subcellular protein fractions from wild-type and *DMD* ko HeLa cells. Full-length blots are provided in Supplementary Original Data.

(c) Immunofluorescence of FLAG-tagged DP71 splice variants in *DMD* ko HeLa and HEK293 cells, with or without *UTRN*knockdown. Image acquisition settings were adjusted to avoid signal saturation and ensure detection of low-abundance variants.

In **a** and **c**, the images were generated from six separate pictures taken at different z–positions. Scale bars: 50 µm.

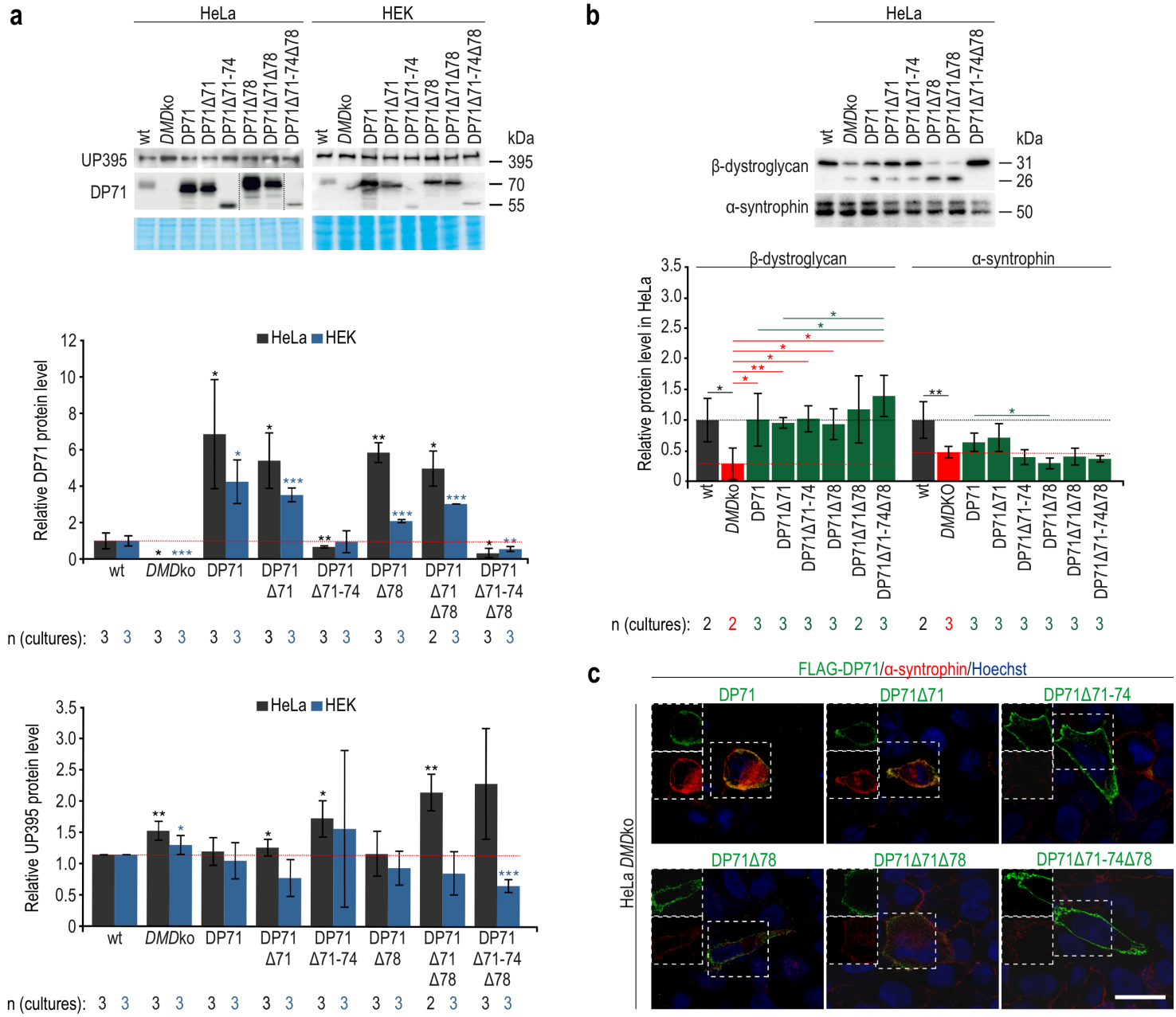


Figure 5

Exons 71–74 are required for DP71 stability and interaction with a–syntrophin.

(a, b) Immunoblot analyses of protein levels in *DMD*ko HeLa and HEK293 (**a**) or HeLa (**b**) cells following transfection with plasmids encoding FLAG-tagged DP71 splice variants. As controls, wt and *DMD*ko cells transfected with an empty FLAG vector were used. Densitometric evaluation of band intensities was performed relative to wt samples with a FLAG-tag. Dashed lines in **a** indicate rearranged membrane fragments (see Supplementary Original Data).

(c) Immunostaining for FLAG-DP71, a-syntrophin, and nuclei (Hoechst) in the *DMD* ko HeLa cell line after administration of various *DP71* vectors. For each image, the microscope z–position was chosen based on the a-syntrophin localisation, and the same parameters were set for all images. Dashed boxes

indicate fragments shown as insets on the left side of each image with the green and red channels separated, allowing for a better visualization of the amount and location of DP71 and syntrophin protein. Scale bar: 50 µm.

The data are presented as mean ± SD. n, number of biological replicates. *, p < 0.05; **, p < 0.01; ***, p < 0.001 (two-tailed unpaired t–test).

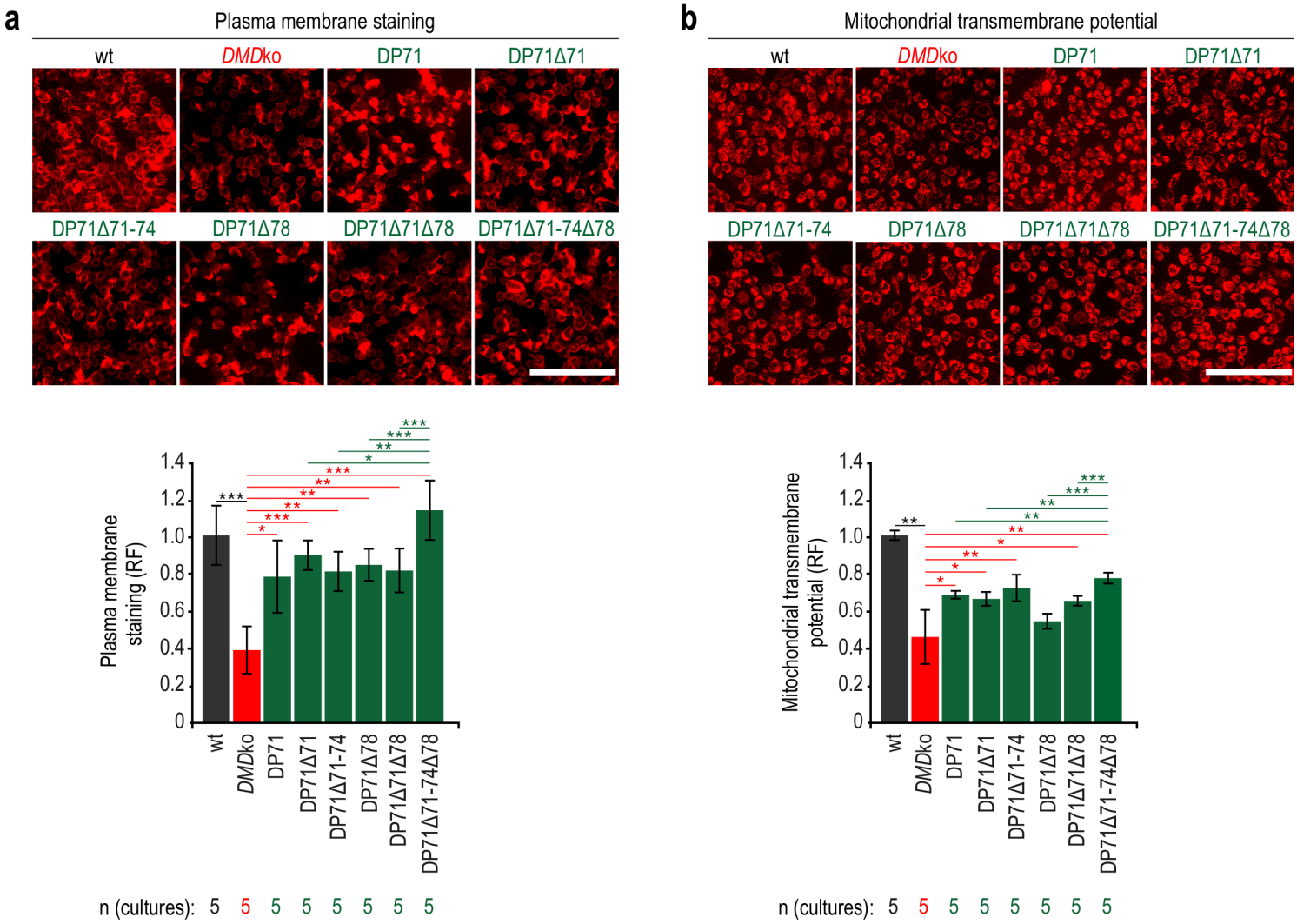


Figure 6

DP71 splice variants differentially restore membrane integrity and mitochondrial function.

(a, **b)** Quantification of cell plasma membrane staining (**a**) and mitochondrial transmembrane potential (**b**) in *DMD*ko HeLa cells following expression of *FLAG-DP71* variants. As controls, wt and *DMD* ko cells with a vector encoding a FLAG tag were used. Quantification was based on fluorescence intensity measurements normalized to Hoechst signal.

Scale bars: 100 µm. The data are presented as mean ± SD. RF, relative fluorescence; n, number of biological replicates. *, p < 0.05; **, p < 0.01; ***, p < 0.001 (two-tailed unpaired t–test).

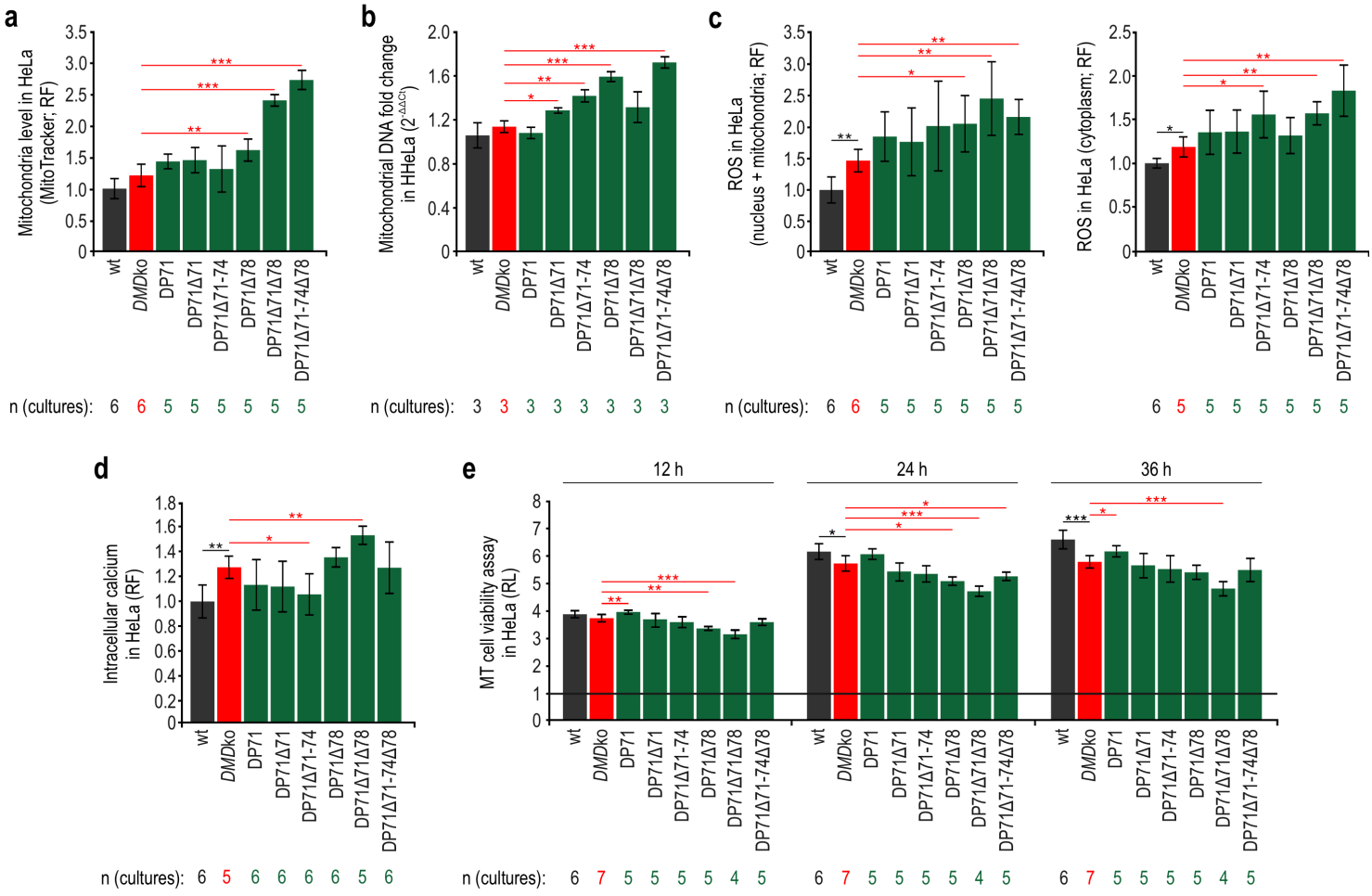


Figure 7

DP71 splice variants differentially affect mitochondrial activity, ROS production, calcium homeostasis, and cell viability.

(a–d) Quantification of active mitochondria (**a**), mitochondrial DNA levels (**b**), ROS production (**c**), and intracellular calcium levels (**d**) in *DMD* ko HeLa cells after delivery of vectors encoding FLAG-tagged DP71 splice variants.

(e) Cell viability following expression of *DP71*variants. As controls, wt and *DMD* ko cells with a vector encoding a FLAG tag were used. The data were quantified based on the Tecan values normalized to the Hoechst signals.

The data are presented as mean ± SD. RF, relative fluorescence; RL, relative luminescence; n, number of biological replicates. *, $p < 0.05$; **, $p < 0.01$; ***, $p < 0.001$ (two-tailed unpaired t–test).

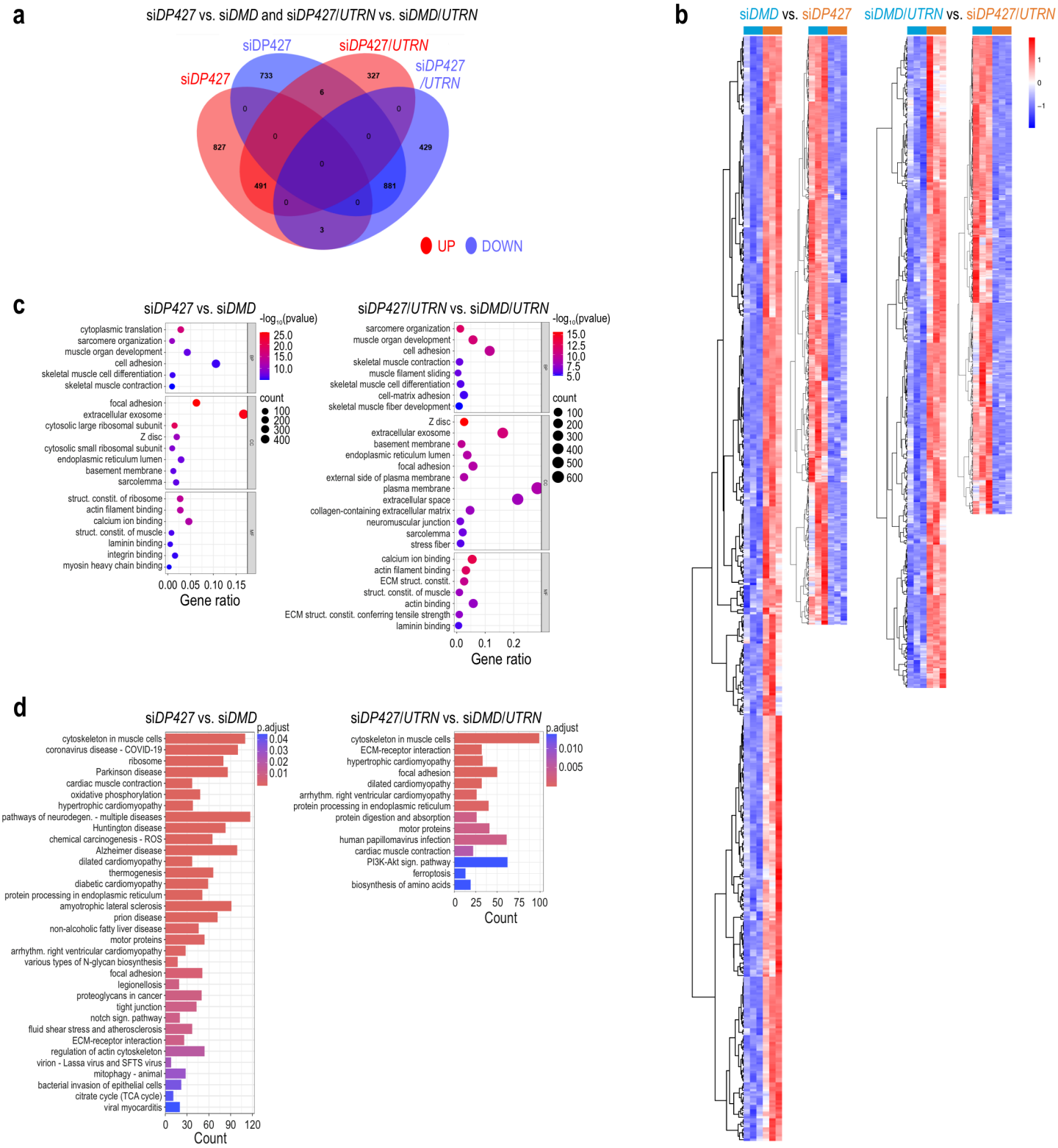


Figure 8

DP71-associated transcriptional responses distinguish DP427-deficient from complete dystrophin-deficient myotubes.

(a) Numbers of upregulated (red) and downregulated (blue) genes in differentiated (d12) HSkM myotubes following siRNA treatment. Venn diagrams show shared and unique gene sets. Differential

expression was determined using Wald test with Benjamini–Hochberg correction (FDR ≤ 0.05).

(b) Heatmaps of normalized expression values for selected gene sets (log2FC > 0.5, adjusted p < 0.05).

(c) GO enrichment analysis of differentially expressed genes. Dot size reflects the number of enriched genes, and colour indicates significance as –log10(p-value). BP, biological process; CC, cellular component; MF, molecular function.

(d) KEGG pathway enrichment analysis of differentially expressed genes. Bar plots show significantly enriched pathways ranked by gene count, with colour indicating adjusted p–value.

Supplementary Files

This is a list of supplementary files associated with this preprint. Click to download.

- Graphicalabstract.tif
- SzwecetalSupplementaryFile.pdf
- DatasetS1siDMDvssiCtrl.xlsx
- DatasetS2siDP427vssiCtrl.xlsx
- DatasetS3siDP427vssiDMD.xlsx
- DatasetS4siDMDandsiUTRNvssiCtrl.xlsx
- DatasetS5siDP427andsiUTRNvssiCtrl.xlsx
- DatasetS6siDP427andsiUTRNvssiDMDandsiUTRN.xlsx